



# Adaptation of transgene mRNA translation boosts the anticancer efficacy of oncolytic HSV1

Huy-Dung Hoang,<sup>1,2,3</sup> Aida Said,<sup>1,2,3</sup> Nasana Vaidya,<sup>4</sup> Victoria H Gilchrist,<sup>1,2,3</sup> Kyle Malone,<sup>1,2,3</sup> Usha Kabilan,<sup>1,2,3</sup> Serena Topshee,<sup>1,2,3</sup> Xiao Xiang,<sup>1,2,3</sup> An-Dao Yang,<sup>1</sup> David Olagner,<sup>5</sup> Karen Mossman,<sup>6</sup> Shawn T Beug,<sup>1,2,3</sup> Seyed Mehdi Jafarnejad,<sup>7</sup> Samuel T Workenhe ,<sup>8</sup> Tyson E Graber,<sup>1</sup> Tommy Alain <sup>1,2,3</sup>

**To cite:** Hoang H-D, Said A, Vaidya N, *et al.* Adaptation of transgene mRNA translation boosts the anticancer efficacy of oncolytic HSV1. *Journal for ImmunoTherapy of Cancer* 2023;**11**:e006408. doi:10.1136/jitc-2022-006408

► Additional supplemental material is published online only. To view, please visit the journal online (<http://dx.doi.org/10.1136/jitc-2022-006408>).

Accepted 03 March 2023

## ABSTRACT

**Background** Transgenes deliver therapeutic payloads to improve oncolytic virus immunotherapy. Transgenes encoded within oncolytic viruses are designed to be highly transcribed, but protein synthesis is often negatively affected by viral infection, compromising the amount of therapeutic protein expressed. Studying the oncolytic herpes simplex virus-1 (HSV1), we found standard transgene mRNAs to be suboptimally translated in infected cells.

**Methods** Using RNA-Seq reads, we determined the transcription start sites and 5'leaders of HSV1 genes and uncovered the US11 5'leader to confer superior activity in translation reporter assays. We then incorporated this 5'leader into GM-CSF expression cassette in oncolytic HSV1 and compared the translationally adapted oncolytic virus with the conventional, leaderless, virus *in vitro* and in mice.

**Results** Inclusion of the US11 5'leader in the GM-CSF transgene incorporated into HSV1 boosted translation *in vitro* and *in vivo*. Importantly, treatment with US11 5'leader-GM-CSF oncolytic HSV1 showed superior antitumor immune activity and improved survival in a syngeneic mouse model of colorectal cancer as compared with leaderless-GM-CSF HSV1.

**Conclusions** Our study demonstrates the therapeutic value of identifying and integrating platform-specific *cis*-acting sequences that confer increased protein synthesis on transgene expression.

## BACKGROUND

The use of viruses to deliver therapeutic payloads is becoming increasingly important in various biomedical applications such as viral vector-based vaccines, gene therapies, and oncolytic viruses (OVs).<sup>1–3</sup> In the case of OVs, high intratumoral transgene expression is crucial to elicit optimal antitumor immune responses<sup>4</sup> and therapeutic efficacy.<sup>5,6</sup> Consequently, OV platforms in clinical and preclinical development are engineered to encode one or more of the following: (1) immunomodulatory host proteins or tumor-associated

## WHAT IS ALREADY KNOWN ON THIS TOPIC

⇒ Oncolytic viruses are armed with transgenes that code for critical therapeutic payloads, but could the expression of these payloads during infection be further improved by optimizing mRNA translation?

## WHAT THIS STUDY ADDS

⇒ We report here that adding a viral 5'leader to the transgene mRNA enhances translation and boosts payload expression in infected cells, ultimately resulting in improved viral-mediated antitumor efficacy.

## HOW THIS STUDY MIGHT AFFECT RESEARCH, PRACTICE OR POLICY

⇒ Tailoring transgene mRNA translation encoded within oncolytic viral platform should be considered in the design of future transgene-armed oncolytic viruses.

antigens that can amplify antitumor immune responses, (2) suicide proteins intended to induce cancer cell death, and/or (3) reporter proteins that facilitate tracking and dosing (e.g., green fluorescent protein or luciferase).<sup>7–10</sup>

The components of a transgene expression cassette incorporated into a viral vector typically encode the transgene as an intronless open reading frame (ORF—encoding the desired therapeutic payload) flanked by an upstream promoter and ended with a poly(A) signal.<sup>11</sup> Remaining sequences from the multiple cloning sites (MCS) between the transcription start site (TSS) following the promoter and the start codon, or the stop codon and poly(A) signal, act as short 5'UTR and 3'UTR, respectively. Much effort is spent on ensuring high transgene transcription in infected cells by incorporating a strong host promoter such as those from



© Author(s) (or their employer(s)) 2023. Re-use permitted under CC BY-NC. No commercial re-use. See rights and permissions. Published by BMJ.

For numbered affiliations see end of article.

## Correspondence to

Dr Tommy Alain;  
[tommya@arc.cheo.ca](mailto:tommya@arc.cheo.ca)

human phosphoglycerate kinase (PGK) or elongation factor 1 $\alpha$  (EF1 $\alpha$ ), or from viruses such as the cytomegalovirus (CMV) immediate early promoter.<sup>11</sup> However, any bottlenecks in the subsequent translation of the transgene mRNA into protein have not been thoroughly investigated under the assumption that differences in the rate of translation would be nominal if the transcript is highly expressed. The innate antiviral response to the presence of replicating viruses challenges this assumption; dramatic changes in the subset of translated mRNAs are observed in infected cells, with replicating viruses actively reshaping the host protein synthesis machinery to favor the production of viral proteins while impeding those of their host.<sup>12,13</sup> Thus, the translation rate of non-viral transgene mRNAs is likely to be altered in infected cells. Ultimately, this could result in suboptimal transgene protein production and consequently compromise the therapeutic potential of the oncolytic viral therapy. An example is the expression cassette of GM-CSF in T-Vec: in a phase I clinical trial, detected GM-CSF levels from fine needle aspirates of several different tumor types plateaued or fell below detection at a mid-range dose, suggesting that expression is suboptimal in humans.<sup>14</sup> In another phase I trial, a clinical oncolytic vaccinia virus candidate also engineered to express GM-CSF, Jennerex-594 (JX594), failed to elicit detectable GM-CSF with low doses of intravenously injected virus ( $10^5$ – $10^6$  viral plaque-forming units; pfu per kg); in stark contrast, an order of magnitude increase in viral dose yielded a positive detection of this therapeutic protein.<sup>15</sup> The requirement to increase dosing is, however, inopportune, as it is desirable to minimize viral dose to improve the safety profiles of these promising viral therapies. In other words, there is a want to increase the specific activity of an OV, enhancing the targeting and expression of its transgene(s) while reducing the accompanying toxic effects of its vector.

Recent studies revealed various translation enhancer motifs found in the 5'leader sequences of viral mRNAs, including non-templated poly(A) leaders in poxviruses<sup>16,17</sup> or ICP27-interacting motifs in herpes simplex virus-1 (HSV1) mRNA 5'leaders that facilitate nuclear export.<sup>18,19</sup> Viral internal ribosome entry sites such as those based on encephalomyocarditis virus (EMCV) are also used in recombinant gene expression to enhance translation of downstream ORFs.<sup>20</sup> However, the inclusion of translation enhancers has not been reported for clinically relevant OVs, including oncolytic poxviruses and HSV1. For example, T-VEC GM-CSF expression cassette does not contain a functionally authentic viral 5'leader, but residual cloning sequences of approximately 100bp originating from the MCS of the plasmid pcDNA3 used in the cloning process.<sup>21</sup> We reasoned that the synthesis of therapeutic payloads from replicating oncolytic platforms may be enhanced by the incorporation of a viral 5'leader. Using RNA-Seq data of HSV1-infected cancer cells, we sought to identify HSV1 5'leaders that mediate high translation efficiency of downstream cistron mRNAs during

viral replication. The 5'leader of the HSV1 late gene US11 increased translation of a downstream cistron in heterologous reporter constructs and, notably, this effect was only observed with concomitant HSV1 infection. HSV1 engineered to express a cassette containing the US11 5'leader upstream of the GM-CSF ORF conferred superior GM-CSF protein expression in several mammalian cell lines and dramatically improved antitumor efficacy and prolonged survival *in vivo* compared with its leaderless counterpart. Our study thus presents an opportunity to enhance therapeutic payload protein expression from oncolytic HSV1 platforms by incorporating a viral 5'leader into the expression transgene cassette.

## METHODS

### Cell culture and viruses

The mouse breast cancer cell line 4T1, mouse colon cancer carcinoma CT26, human prostate cancer DU145, human renal carcinoma 786-O, HEK293T and Vero cells were acquired from American Tissue Culture Collection. 4T1 was maintained in Roswell Park Memorial Institute (RPMI) 1640 (Fisher) supplemented with 10% fetal bovine serum (FBS) (Sigma-Aldrich) and 1X penicillin/streptomycin (Fisher). HEK293T and Vero cells were maintained in Dulbecco's Modified Eagle Medium (DMEM) (Fisher) supplemented with 10% FBS and 1X penicillin/streptomycin (Fisher). Cells were incubated at 37°C, 5% CO<sub>2</sub> v/v. HSV1716 (HSV1 strain 17 with  $\gamma$ 34.5 deleted, Sorrento Therapeutics) was kindly provided by the manufacturers. HSV1 strain KOS was kindly gifted by Dr Karen Mossman. All HSV1 strains were propagated in Vero cells. A monolayer of Vero cells was inoculated with HSV1 at 0.1 MOI, then cultured for approximately 24–48 hours until close to 100% cytopathic effect was observed. Supernatant was then collected separately, and infected cells were freeze-thawed three times to release intracellular virus. Both the cultured supernatant and the freeze-thawed lysate were clarified by centrifugation at 1000g, 5min to remove cell debris. The supernatants were combined and filtered through a 0.45  $\mu$ m filter. Virus particle was further purified using a sucrose cushion by overlaying the supernatant on top of a 36% sucrose cushion in PBS and centrifuged at 18000g for 2 hours, 4°C. Virus in the pellet was resuspended in HNE buffer (HEPES 10mM, NaCl 150mM, EDTA 0.1mM, pH 7.2) and stored at –80°C.

### RNA-Seq mapping and TSS identification

RNA-Seq data of 4T1 cells infected by HSV1 was previously published.<sup>22</sup> For mapping of RNA-seq, RNA reads were mapped to the HSV1 reference genome JQ780693.1 using HISAT2.<sup>23</sup> Only one copy of the two flanking inverted repeat regions were used: the TRL region 1-8870 and TRS region 144602-151023 were omitted. TSS was manually identified from RNA read coverage, defined by an abrupt increase of read coverage at a base position (shown in figure 1f). The leader sequence was defined as

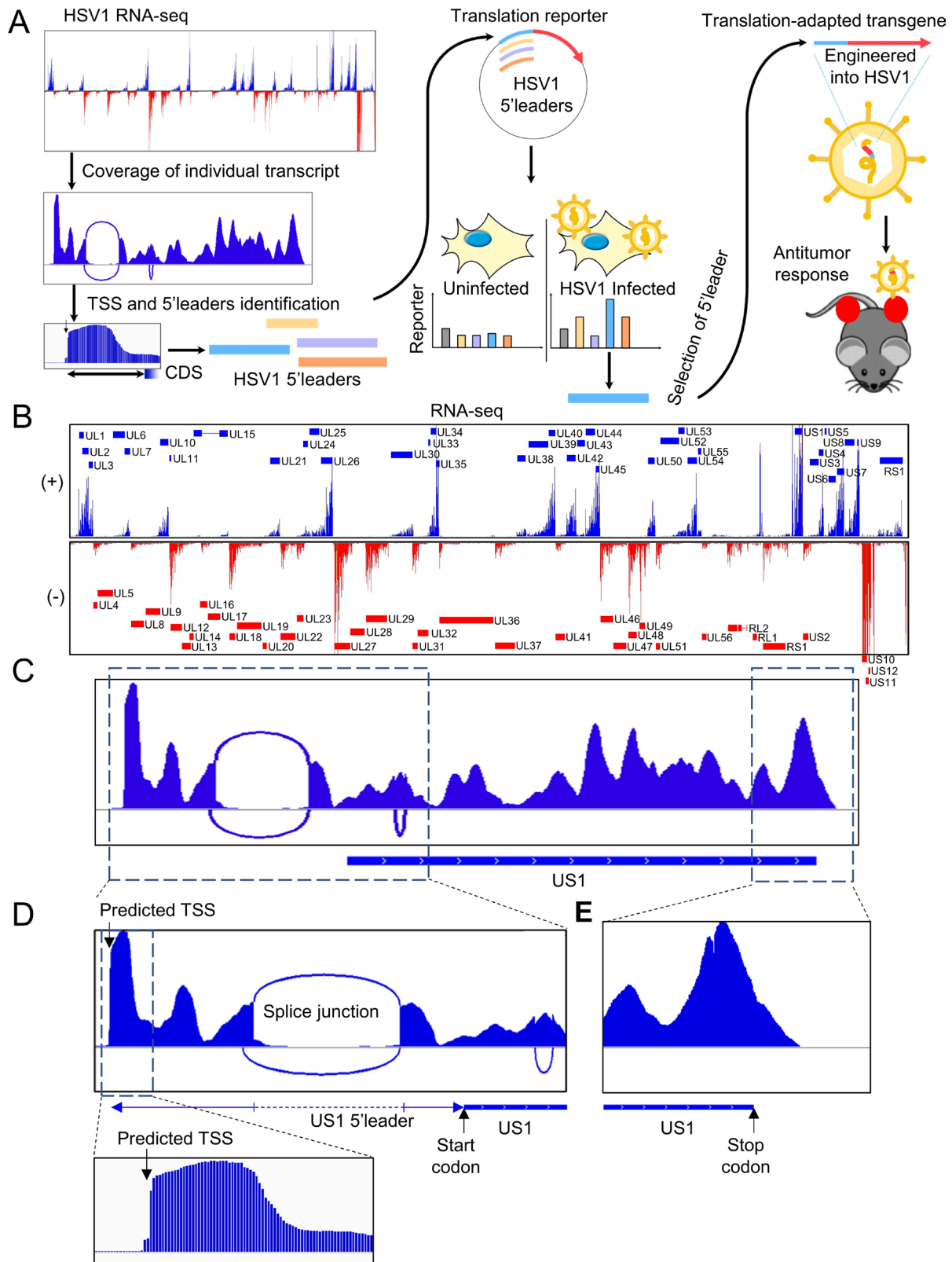


**Figure 1** Characterizing HSV1 individual transcript from RNA-seq coverage. (A) Schematic overview of the workflow to identify HSV1 5'leaders from RNA-seq read, screen for translation enhancing 5'leaders specifically in HSV1-infected cells, and incorporate the 5'leader into transgene expression in an oncolytic HSV1 genome to test in a tumor model *in vivo*. (B) Total RNA-seq coverage of the HSV1 genome from 4T1 infected cells. Strand-specific RNA reads were mapped to HSV1 genome and separated by strand direction to avoid ambiguous mapping of overlapping genes. (C) RNA-seq coverage of the US1 gene. Intron-spanning reads were also detected and shown using Sashimi plot. (D) RNA-seq coverage in the 5' region of US1 gene. Lower plot shows the region of the predicted TSS at nucleotide resolution. (E) RNA-seq coverage at the 3' region of US1 gene. TSS, transcription start site.



the sequence from the TSS to the annotated start codon of the associated HSV1 gene, excluding any spliced intron if applicable. For converting leader sequence coverage between different HSV1 reference genomes (JQ780693.1 to JN555585.1), the sequence of the identified leader from JQ780693.1 was aligned to JN555585.1 using NCBI-BLAST to find the corresponding coordinates on JN555585.1. Raw data were deposited and analyzed on the Galaxy server.<sup>24</sup> Gene expression level from mapped RNA-seq and Ribo-seq reads was calculated using Cuffdiff.<sup>25</sup>

### Plasmid construction

For the leader translation activity screen using the CAT reporter assay, virus leader sequences were amplified by PCR from cDNA reverse-transcribed from mRNA of HSV1 infected 4T1 cells. Briefly, total RNA was extracted from cell using TRIzol reagent (Fisher), treated with Turbo DNA-free kit (Thermo Fisher) to remove potential contamination of virus genomic DNA, then reverse-transcribed by using the iScript Advanced cDNA Synthesis Kit (BioRad). The forward and reverse primers (NotI\_5'UTR-F and XhoI\_5'UTR-R) of each leader also contain the restriction sites of NotI and XhoI, respectively, for subsequent cloning. Amplification specificity was confirmed for each pair of primers by including a negative control cDNA from mRNA of uninfected 4T1. The PCR amplicons were cloned into the CAT reporter plasmid pMCpA (a kind gift from Dr. Martin Holcik, Carleton University) using the NotI-XhoI restriction sites.<sup>26</sup> A leaderless CAT reporter construct, in which only a short residual sequence from the plasmid MCS is transcribed with the CAT CDS, was used as control (this residual sequence also present in all viral 5'leader construct, directly 5' upstream of the leader sequence). For inserting transgene expression cassette into HSV1 genome, the cassette was cloned into the pTK-Green plasmid,<sup>27</sup> flanked by two regions of the HSV1 TK gene to allow for homologous recombination. The expression cassette consists of the leader, followed by the transgene (firefly luciferase or mouse GM-CSF), the self-cleaving peptide porcine teschovirus-1 2A (P2A) and GFP. The insert was generated by fusion PCR. The virus leader was amplified as described above using a forward primer containing an AgeI cutting site (AgeI\_5'UTR-F) and a reverse primer with an overlap section of the transgene 5'end (5'UTR\_LUC-R or 5'UTR-CSF2-R). The second fragment containing the transgene CDS was amplified using a forward primer (5'UTR\_LUC-F or 5'UTR-CSF2-F), and a reverse primer consisting of the CDS 3' end, a GSG linker and a part of the P2A sequence (LUC-GSG-P2A-R). The third fragment containing the GFP was amplified using a forward primer (GSG-P2A-GFP-F) and a reverse primer that included a KpnI cutting site (GFP-KpnI-R). All three fragments were purified using the QIAquick PCR Purification Kit (Qiagen), then used as templates for fusion PCR using the 5'-most (AgeI\_5'UTR-F) and 3'-most primer (GFP-KpnI-R). The resulting PCR product was cloned into the pTK-Green using AgeI and XhoI sites. A

leaderless LUC-GFP or CSF2-GFP construct, in which only a short residual sequence from the plasmid MCS is transcribed with the transgene CDS, was used as control (this residual sequence was also present in all viral 5'leader constructs, directly 5' upstream of the leader sequence). All plasmids were verified by Sanger sequencing. All primer sequences are presented in online supplemental table S1.

### CAT reporter assay

CAT reporter assay was performed as previously described.<sup>22</sup> Cells were seeded at approximately 75% confluency in a 6-well plate and incubated for 1 day before transfection. In the case of HSV1 infection, cells were infected with HSV1 at 5 MOI 1 hour before transfection. CAT reporter plasmid was co-transfected with  $\beta$ -Galactosidase plasmid (pBGal, a kind gift from Dr. Martin Holcik, Carleton University<sup>26</sup>) at 1  $\mu$ g per each plasmid using Lipofectamine 2000 (ThermoFisher) according to the manufacturer's protocol. Cells were lysed 24 hours post-transfection and assayed for CAT expression using the CAT ELISA kit (Roche).  $\beta$ -Galactosidase activity was also measured from lysate using ortho-Nitrophenyl- $\beta$ -galactoside colourimetric assay. CAT expression was normalized to  $\beta$ -Galactosidase activity to control for transfection efficiency.

### Quantitative RT-PCR

DNase-treated RNA and cDNA were prepared as described above. For RT-qPCR, SsoAdvanced Universal SYBR Green supermix (BioRad) was used with a CFX96 Touch Real-Time PCR Detection System (BioRad). The PCR condition was 95°C for 3 min, followed by 40 cycles of 95°C for 10 s and 60°C for 30 s, and ended with a standard melting curve cycle. Gene expression was calculated using the  $\Delta\Delta$ Ct method against the indicated reference genes. The list of primers for the genes or sequences of interest is in online supplemental table S1.

### Western blot

Cells were washed once with 1X PBS, then lysed on ice using RIPA buffer (150 mM NaCl, 1.0% IGEPAL CA-630, 0.5% sodium deoxycholate, 0.1% SDS, 50 mM Tris, 50 mM NaF, 15 mM NaVO<sub>3</sub>, pH 8.0) supplemented with cComplete Protease Inhibitor Cocktail (Roche). Lysate was centrifuged at 10,000 g, 10 min at 4°C to remove cell debris. Protein concentration was determined using the DC Protein assay kit (BioRad). An indicated amount of total protein was used for SDS-polyacrylamide gel electrophoresis (PAGE) using 10% SDS-polyacrylamide gel. Separated protein was transferred to PVDF membrane; the membrane was blocked with 5% w/v skim milk in TBST buffer (10 mM Tris, 50 mM NaCl, 0.1% Tween-20, pH 7.5) and then blotted for the indicated antibody. The following antibodies and corresponding dilution were used: anti-GFP (Abclonal, CAT#AE011) at 1:2000, anti- $\beta$ -actin (Sigma, #A5441) at 1:10,000, IRDye 800CW Goat anti-Mouse IgG Secondary Antibody (LICOR,

CAT#926-32210) at 1:20,000 and IRDye 680RD Goat anti-Rabbit IgG Secondary Antibody (LICOR, CAT#926-68071) at 1:20,000.

### Live-cell monitoring of GFP expression

Live-cell monitoring of GFP expression was performed using the IncuCyte Live-Cell Monitoring system (Sartorius). Transfection and/or infection were performed as indicated, then cell plates were placed inside the IncuCyte system and cultured and monitored at 37°C, 5% CO<sub>2</sub> with phase contrast and fluorescent images taken every 2 hours. Images were analyzed with the IncuCyte ZOOM software using the following parameters: background subtraction using Top-Hat method (disk shape structuring element with radius of 10 µm, threshold of 1.0 green calibrated unit), edge split: Off, Hole Fill: No, Adjust Size: No, Filters: No.

### Generating recombinant HSV1 viruses

For inserting the expression cassette into HSV1 genome, we targeted the TK gene for insertion as previously described.<sup>27</sup> HSV1 genomic DNA was extracted from purified virus stock using the QIAamp DNA mini kit (Qiagen). HEK293T cells were seeded at 75% confluency 1 day before in six-well plates and then co-transfected with HSV1 gDNA:pTK-Green plasmid at a ratio of 1:40, for a total amount of 1 µg DNA/well, using Lipofectamine 2000 (Thermo Fisher) according to manufacturer protocol. Cells were then cultured for 3–5 days until cytopathic effect was observed. Cells were then freeze-thawed three times, centrifuged at 1000 g, 5 min to remove cell debris and supernatant was collected. Supernatants at various dilutions were then inoculated to a monolayer of Vero cells in order to separate individual plaques overlaid with DMEM supplemented with 10% FBS and 1% carboxymethylcellulose (CMC) to allow for the development of individual plaques. GFP-positive plaques were selected and subjected to multiple plaque purification rounds until a pure GFP-expressing HSV1 population was obtained. Insertion of the cassette into HSV1 genome was confirmed first by PCR genotyping using a forward primer on the TK gene (pTK-seq) and a reverse primer on the transgene (CSF2.e-R), followed by Sanger sequencing.

### Plaque titration

Virus stock or solution was serially diluted, then inoculated a monolayer of Vero cells and incubated for 1 hour, 37°C, 5% CO<sub>2</sub> with frequent shaking. The virus-containing media was then removed and an overlay of DMEM + 10% FBS + 1% agar was added. Cells were then cultured at 37°C, 5% CO<sub>2</sub> until visible plaques could be observed using a brightfield microscope. Plaques were visualized using crystal violet staining and counted.

### Polysome fractionation

Polysome fractionation was performed as previously described.<sup>28</sup> Briefly, cells were treated with cycloheximide (CHX) (Bioshop, CAT #66-81-9) at 100 µg/mL for 5 min to stop ribosomes, washed three times with ice-cold PBS

supplemented with CHX (100 µg/mL) and lysed using polysome lysis buffer (5 mM Tris pH 7.5, 2.5 mM MgCl<sub>2</sub>, 1.5 mM KCl, 100 µg/mL CHX, 2 mM DTT, 0.5% Triton X-100, 0.5% sodium deoxycholate) supplemented with 100 units RNasin Ribonuclease inhibitor (Promega). Cell debris was cleared by centrifugation at 14,000 g for 10 min, 4°C. Supernatant was then loaded on a 10%–50% continuous sucrose gradient and centrifuged at 36,000 rpm, 90 min at 4°C in an SW41Ti rotor. Fractions were then collected, and the OD260 absorbance of fractions was monitored using a Brandel Fraction Collector System (Brandel). RNA was extracted from each fraction using TRIzol reagent (Thermo Fisher) according to the manufacturer's protocol.

### GM-CSF quantification

To measure GM-CSF production from engineered HSV1 infection, cells were seeded at 80%–90% confluency and then infected with the indicated HSV1 at a MOI of 5. 24 hours postinfection, culture supernatant was collected and GM-CSF production was measured using the Mouse GM-CSF ELISA Kit (CSF2) (Abcam, CAT #ab100685) according to the manufacturer's protocol.

### Single step-growth curve and monitoring HSV1 genes expression

For monitoring virus replication and viral gene transcription during a single-step growth curve, cells were seeded at 80%–90% confluency and infected the next day at a MOI of 5. Both cells and culture supernatant were collected at the indicated time points and used for virus titration by plaque assay or RNA extraction for quantification of viral transcript expressions as described above.

### CT26 subcutaneous tumor model

Female BALB/c were ordered from Charles River (Kingston, New York, USA). Animals were received at 5–6 weeks old, housed at 5 per cage, fed ad libitum, and acclimated to the facility for 2 weeks before experimental manipulation. For tumor implantation, 10<sup>5</sup> CT26 cells were injected subcutaneously into both flanks of the mouse. When tumors were palpable (~5×5 mm), the tumor on one flank was injected twice, 1 day apart, intratumorally with 50 µL DMEM or 5×10<sup>5</sup> PFU of the indicated virus, while the tumor on the other flank was left untreated (contralateral). Tumor sizes were measured every 2 days using a caliper. Animals were euthanized when an individual tumor reached 2000 mm<sup>3</sup>, or at an alternate humane endpoint. The *in vivo* study was done single-blinded: the animal handler did not know the treatment given to each mice group. For assessing intratumoral GM-CSF level and HSV1 transcript abundance, tumors were excised and homogenized in PBS buffer using 2.0 mm zirconia beads (Thomas Scientific, CAT # 1197P96) with a TissueLyzer II (QIAGEN) at 20 Hz/s. Half of the homogenate was used for measuring GM-CSF using the Mouse GM-CSF ELISA Kit (CSF2) (Abcam, CAT #ab100685) according to the manufacturer's protocol.

The other half of the homogenate was used for RNA extraction with Trizol Reagent (Thermo Fisher), and then the transcript mRNA was quantified by RT-qPCR as described above.

### IFN $\gamma$ ELISPOT assay

Splenocytes were isolated freshly from spleens of mice 8 days after the first injection and cultured in RPMI (Fisher) supplemented with 10% FBS (Sigma-Aldrich) and 1X penicillin/streptomycin (Fisher). IFN $\gamma$  ELISPOT was done using the mouse interferon-gamma ELISPOT kit (Abcam, CAT# ab64029) according to the manufacturer's protocol. Briefly, 100,000 splenocytes were co-cultured with/without 50,000 UV-irradiated CT26 in the ELISPOT well for 24 hours. Cells were then thoroughly washed away from the well, and IFN $\gamma$  spots from stimulated T-cells were developed. Individual wells were imaged using the stereomicroscope LEICA EZ4 W, and spots were counted manually.

### Data and code availability

The RNA-seq data were published previously<sup>22</sup> and are available on the NCBI Gene Expression Omnibus (GEO: GSE137757), sample IDs GSM4086602 and GSM4086610 (HSV1 infected mRNA replicate).

### Statistical analyses

All experiments were performed in at least three biological replicates. Statistical analyses were performed using GraphPad Prism V.8, using the method indicated in figure legends. Error bars indicate SD. \* $p < 0.05$ , \*\* $p < 0.01$ , \*\*\* $p < 0.001$ , \*\*\*\* $p < 0.0001$ , ns, non-significant.

## RESULTS

### Determining HSV1 mRNA 5'leader sequences

HSV1 is an enveloped dsDNA virus with a 153 Kb genome arranged in covalently linked long (L) and short (S) segments that collectively encode approximately 80 genes.<sup>29</sup> Several single-gene studies identified and characterized the 5'leaders and 3'untranslated regions (3'UTRs) of a limited number of HSV1 genes<sup>30–36</sup> (see table 1). Most transcripts, however, have no such annotations in the public NCBI database (e.g., NCBI accession number JQ780693 for strain KOS and JN555585 for strain 17). We previously generated RNA-Seq data of HSV1 infected 4T1 murine breast cancer cells.<sup>22</sup> The HSV1 reads from this RNA-seq data can be used to identify and assess translationally active 5'leader (figure 1A). By mapping the HSV1 reads from this dataset to the KOS strain reference genome (JQ780693.1), we can distinguish RNA transcripts originating from each of the positive and negative gDNA strands (figure 1B). We can also discern the splice junctions of the four known spliced transcripts of HSV1 (i.e., UL15, US1, US12 and RL2) and the intron retention that was previously reported for RL2 (online supplemental figure 1).<sup>37</sup>

Identification of transcription start sites (TSS) from long-read sequencing techniques (e.g., PacBio methods)<sup>38</sup> or full transcript sequencing (e.g., Oxford Nanopore MinION platform)<sup>39</sup> can be more straightforward than RNA-Seq that relies on aligning short reads, especially when there are overlapping ORFs present. However, we found that standard RNA-Seq read mapping can sufficiently identify the TSS for HSV1 genes. We scored TSS locations by monitoring for a 'wall' of stacked short reads that we interpreted as the start of a transcript (figure 1C,D). Whisnant *et al* have recently used a similar strategy to enumerate the HSV1 TSS, though their methods require more specialized RNA-Seq methods.<sup>40</sup> We detected reads that flanked the 5' and 3' ends of most annotated ORFs (figure 1D,E, respectively), confirming that all annotated HSV1 transcripts harbor both a 5'leader and a 3'UTR. Although the 3'UTRs of a large portion of the viral genes overlapped with a downstream ORF, a spike in read density at a single nucleotide position upstream of the start codon consistent with a TSS could be clearly distinguished across 5'leaders (figure 1C, insets and table 1, the read density coverage at each identified TSS are shown in online supplemental figure 2). Using these TSS coordinates, we identified 61 5'leader sequences of HSV1 genes (table 2). Importantly, when comparing the identified TSSs with the few annotated in NCBI, more recently identified by long-read sequencing done by Tombácz *et al*,<sup>38</sup> or RNA-Seq on enriched 5' end reads by Whisnant *et al*,<sup>40</sup> we found that the coordinates of the TSSs were exact or differed by only a few nucleotides (table 1). These studies confirmed our approach to robustly detect and confidently annotate each HSV1 transcript 5'leader.

### The US11 5'leader enhances the translation of downstream ORFs in HSV1-infected cells

Having identified the 5'leader sequences of most HSV1 genes *in silico*, we next sought to determine their ability to modify the translation output of a downstream cistron. We hypothesized that the 5'leaders of HSV1 late genes expressed in an established infection stage should be best adapted to the altered translation control of HSV1 infection. We selected ten late genes for testing the translation modification effect of their 5'leader in HSV1 infected cells (online supplemental figure 3).<sup>41</sup> HSV1 5'leaders of selected late genes were amplified from a cDNA library generated from HSV1-infected 4T1 cells and inserted upstream of the chloramphenicol acetyltransferase (CAT) reporter construct<sup>42</sup> (figure 2A and online supplemental figure 4A). We performed the translation reporter assay under uninfected and HSV1-infected conditions by cotransfecting 4T1 cells with monocistronic plasmids expressing CAT and  $\beta$ -galactosidase post-infection, the latter construct included to standardize differences in transfection efficiency. In uninfected cells, the viral 5'leaders had both positive and negative effects on reporter expression, though no statistically significant differences were observed (figure 2B). The US11



**Table 1** HSV1 TSS identified in this study (Hoang et al) compared with Tombacz et al<sup>38</sup> and Whisnant et al<sup>40</sup>

Hoang et al (This study)		Tombacz et al				Whisnant et al	
HSV1 Genes	TSS coordinates (JQ780693.1)	5'UTR coordinates (JQ780693.1)	5'UTR length	TSS coordinates (JN555585)	TSS coordinates (JN555585)	Differences to our study (nt)	Differences to coordinates (JN555585)
UL1+	8901	JQ780693.1+:-8901-8994	92	9245	9242	3	9245
UL2+	9396	JQ780693.1+:-9396-9541	145	9740	9739	1	9739
UL3+	X				10736		
UL4-	12151	JQ780693.1+:-12079-12151	72	12495	12494	1	12494
UL5-	X				15581		
UL6+	X				15032		
UL7+	16613	JQ780693.1+:-16613-16792	179	16957	16956	1	16956
UL8-	20337	JQ780693.1+:-20134-20337	203	20680	20677	3	20679
UL9-	X				23358		
UL10+	22601	JQ780693.1+:-22601-22862	261	22944	22943	1	22943
UL11-	25148	JQ780693.1+:-24741-25148	407	25499	25498	1	25498
UL12-	26695	JQ780693.1+:-26537-26695	158	27046	27045	1	27045
UL13-	X				28657		
UL14-	X				29249		
UL15+	28451	JQ780693.1+:-28451-28670	219	28802	28801	1	28801
UL16-	31261	JQ780693.1+:-30949-31261	312	31608	31607	1	31607
UL17-	X				33719		
UL18-	35902	JQ780693.1+:-35704-35902	198	36250	36249	1	36247
UL19-	40421	JQ780693.1+:-40182-40421	239	40768	40768	0	40766
UL20-	X				41613		
UL21+	41515	JQ780693.1+:-41515-41726	211	41863	41862	1	41862
UL22-	46230	JQ780693.1+:-46031-46230	199	46582	46581	1	46581
UL23-	47558	JQ780693.1+:-47451-47558	107	47910	47906	4	47909
UL24+	47008	JQ780693.1+:-47008-47386	378	47360	47671	-311	47407
UL25+	47722	JQ780693.1+:-47722-48461	739	48074	48630	-556	48630
UL26+	50311	JQ780693.1+:-50311-50469	158	50664	50659	5	50663
UL26.5+	51249	JQ780693.1+:-51294-51387	93	51635	51636	-1	51634
UL27-	55744	JQ780693.1+:-55458-55744	286	56081	56080	1	56080
UL29-	61979	JQ780693.1+:-61717-61979	262	62312	62312	0	62313
UL30+	X				62605		

Continued



**Table 1** Continued

Hoang et al (This study)					Tombácz et al		Whisnant et al		
HSV1 Genes	TSS coordinates (JQ780693.1)		5'UTR coordinates (JQ780693.1)	5'UTR length	TSS	TSS	Differences to our study (nt)	Differences to our study (nt)	
					coordinates (JN555585)	coordinates (JN555585)			
UL31-	67123		JQ780693.1:-67044-67123	79	67458	67458	0	67457	1
UL32-	68885		JQ780693.1:-68827-68885	58	69220	69220	0	69219	1
UL33+	68730		JQ780693.1+:68730-68826	96	69065	69065	0	69064	1
UL34+	69107		JQ780693.1+:69107-69298	191	69442	69442	0	69441	1
UL35+	70151		JQ780693.1+:70151-70231	80	70486	70489	-3	70488	-2
UL36-	X					?			
UL37-	83780		JQ780693.1:-83649-83780	131	84215	84215	0	84214	1
UL38+	83958		JQ780693.1+:83958-84088	130	84393	84394	-1	84393	0
UL39+	85774		JQ780693.1+:85774-86000	226	86217	86214	3	86216	1
UL40+	89331		JQ780693.1+:89331-89482	151	89774	89775	-1	89773	1
UL41-	92312		JQ780693.1:-92193-92312	119	92755	92755	0	92753	2
UL42+	924191		JQ780693.1+:92491-92669	178	92934	92936	-2	92934	0
UL43+	94323		JQ780693.1+:94323-94357	34	94765	94653	112	94764	1
UL44+	95723		JQ780693.1+:95723-95865	142	96171	96174	-3	96173	-2
UL45+	95706		JQ780693.1+:95706-97585	79	96154	97953	-1799	97953	-1799
UL46-	X					100995			0
UL47-	102866		JQ780693.1:-102672-102866	194	103312	103311	1	103309	3
UL48-	104814		JQ780693.1:-104635-104814	179	105258	105257	1	105257	1
UL49-	106099		JQ780693.1:-105949-106099	150	106542	106543	-1	106538	4
UL49A-	106686		JQ780693.1:-106551-106686	135	107129	107128	1	107126	3
UL50+	106387		JQ780693.1+:106387-106568	181	106830	106826	4	106829	1
UL51-	108863		JQ780693.1:-108569-108863	294	109306	109305	1	109302	4
UL52+	X					108985			
UL53+	111501		JQ780693.1+:111501-111737	236	111944	111943	1	111943	1
UL54+	113153		JQ780693.1+:113153-113292	139	113596	113598	-2	113598	-2
UL55+	115002		JQ780693.1+:115002-115054	52	115445	115447	-2	115444	1
UL56-	116643		JQ780693.1:-116485-116643	158	117084	117083	1	117083	1
RL2-	123628		JQ780693.1:-123482-123628	146	124258	124256	2	124255	3
RL1-	125310		JQ780693.1:-125206-125310	104	125965	125944	21	125964	1

Continued



Hoang et al (This study)		Tombácz et al			Whisnant et al		
HSV1 Genes	TSS coordinates (JQ780693.1)	5'UTR coordinates (JQ780693.1)	5'UTR length	TSS coordinates (JN555585)	TSS coordinates (JN555585)	Differences to our study (nt)	Differences to coordinates (JN555585) our study (nt)
RS1-	130 404	JQ780693.1+:130103-130404	301	131431	131428	3	131429 2
US1+	131 098		602				0
		JQ780693.1+:131098-131700	354 (spliced)	132128	132127	1	132129 -1
US2-	134 359	JQ780693.1+:133983-134359	376	135307	135306	1	135305 2
US3+	134 019	JQ780693.1+:134019-134277	258	134967	134958	9	134966 1
US4+	135 787	JQ780693.1+:135787-135799	12	136735	136733	2	136734 1
US5+	X				137625		0
US6+	137 395	JQ780693.1+:137395-137476	81	138342	138338	4	138345 -3
US7+	138 754	JQ780693.1+:138754-138843	89	139699	139698	1	139699 0
US8+	140 208	JQ780693.1+:140208-140282	74	141173	141170	3	141171 2
US8A+	141 665	JQ780693.1+:141665-141783	118	142630	142626	4	142629 1
US9+	142 287	JQ780693.1+:142287-142352	65	143252	143250	2	143251 1
US10-	144 183	JQ780693.1+:144114-144183	69	145169	145171	-2	145168 1
US11-	144 480	JQ780693.1+:144265-144480	215	145466	145461	5	145461 5
US12-	145 247	JQ780693.1+:144596-145247	319 (spliced)	146069	146068	1	146066 3



Table 2 Continued

Gene name (strand)	5'leader length	5'leader sequence
UL15+	219	gggtgtgacgcccctcccggtgagctgcagggtgtgtctttaaattctggtcggagggtcgtctcgccaggcgtcggcgc agggccgctggtggcgcatctcgttcattccgccacctcgtggcgacccgggggtgtctctgtagtctcgtcgtgccaaagg cccgtgattcgggtacttcgccgccgacccgcaaccgggtgtgcgcg - atg
UL16-	312	acagccccacgcagggtctgtcagcaataactgtcccgggaaagctacgcctacctctgcctggggtttaatcgcgcgcctgtgg catagttctttccgggcgttgcgttacattacatcgcgcctacctagctctcggaccgcgtcgcgggcgcgtgtctctta gttttgtcgaaggtctcgcgggaacgcggtctcgtctgtagcgggccttccccggccacctcgcgccaccactcctccccg cgcgttgcccccgccctctgggttgccctcccccgccccgcgc - atg
UL17-	222	agccataatcgtctggaccgcctcgggcgaataaagttggcctcgtcgacaaagacaggttaaagtctggcctcggatt cccctagacagaaagaaacgcgccgcataagcacgcacctcgttgcgaaatcgcatacgcgcgccaaacccac gccctccccgcgactcggggacccgcctacacacccacccccgaacc - atg
UL18-	198	ggattcgcctcgtgctctggcccgcagacacctccccgcgcctgtctgggtccctcgtcgcctcccaacccccctaag acccaacccccgtctatgcgaggttgctccgcctctgtctacgcgcctgacccccacgcgcctcctccgcgccaccgaa ccacactgcactccctgcgcgtgcatggcgcc - atg
UL19-	239	ggctgtggggacactgggtctctcctggaacgagcgccagccttccccgtgcctttccccccgcacccggcaccccg cctctcacacagcatccccgcctttttggctccggccgcctgtcttcttggtggacctgggccgtc gggcacgtacacgggt ggccgggcgttggtgggtgatcttagcctccccgggccaatatcgttagacagcgcgatctccacgcgacccc - atg
UL20-	125	actcgcctcgcgcggtgcaccccggtgggtttgtgcaagaacccgggtgtctttgatctcgggattcctgtgacgtaaagcac cctttgcggtttcgtctccccactccacgcacacccc - atg
UL21+	211	tctgttattcagacctgcctgtgcaacgcacgtcgggttgctcgtgtcgcgttgcccccacccgcgtgcgcacgcagga cgagtcgcgtgtcttattggcgttcaagcgttgcctccagttctgtgtcgtgttccccataccacgcgccacatccacgtagg ggccctctgggcgcgtgttaactgcgcgcgcgcgcg - atg
UL22-	199	ataaacgcgggggttcggtccaggctgcactctgtcgataccccacccagagacccattgggaccaatacgcgccgcgtttcttc ttttccccaccacaacccccaaagtccgggtgaaggccagggtcgcagccaacgctcggggcggaagccctgcctagccacg ggccccgtgggttagggacgcgggtcccc - atg
UL23-	107	accgagcgacctcgcgcgacccgcttaacagcgtcaacagcgtccgcgagatcttggtggcgtgaaactccccgcacctctt cggccagcgccctgtagaagcgt - atg
UL24+	378	cccagcctccccccgatagaggagccagacggcgtcggtcacggcataaggcatgccattgttatcttggcgcttgt cattacaaccgcgcgtccccgcggcgtatctacccctggtcagggcgtgtgtgtgtggttagatgttcgcgattgtctcggagc ccccaacacccgccagtaagtcacgcgtcgggtacgtagacgatatctcgcgcgaacccaggggccaccagcagttgcgtgg ttggtgttttccccatcccgctggggacgcgtctatataaacccgcagtagcgtgggcattttctgtctccaggcggacctcgtggttttg ttgcgcgcgagggcgcaacgcgcgtacgtcggttgt - atg

Continued

Table 2 Continued

[illegible]



Table 2 Continued

Gene name (strand)	5'leader length	5'leader sequence
UL38+	130	caacacaacccaccggagggtagccgctttggctgtgggtgggtgggttcgcgcttgctgagtgctcttgcaccaccccccc cctccctcccccggtctgtctaggttcgcgatactggggctcgca - atg
UL39+	226	ccacagggtgggtgctttgaaacttgccggtcgccgtgctctctgtgagcttgctccctcccggttctcttgcgtccgccttcc ggacctgctctgcctactcttttggctctgggtgcgattgctcaggcagcgcttgcgaatctcgaccocaccactgcgcgg accgcgcgacgtccctctcgagcccgccgaaacccgcgcgtctgtgaa - atg
UL40+	151	actactgcaagggttcgaagcgaccaacagcggggcttttggcggcgacgacaacattgtctgcatgagctgcgcgtgtga ccgataaacccctctcgccgacaggcccgccactgtctgcctccacgctctccctgtgcc - atg
UL41-	119	cccttgtctcgggtgtgtctgggtcaccatacacagagacagagctcgggtgtccggacgctgcaccaacaacg ccttagttagccgacgcagttacaattgacctgac - atg
UL42+	178	cgtagtttctggctcgtgagcgacgtccgtctgttctgttggtccctggctgccatcaaaaaacccaccctcgacgcggcatacgt ccccctcgcgtccgcacccgagaccocggcccgctgccctaccacgaagcccactcgtcactgtgggtgttcccagcccgcgttggg - atg
UL43+	34	gtgtatttcttccctgtctataaaagccgt - atg
UL44+	142	ccctcacatatcagggcgcttggctcgggagccgcacatcgaacgcacaccccccatccgggtgtcgtgtgaggtcgttttca tgccgggtctcgtttgcgggaacgctagccgatacctcgcgcgaggggagcgtcgggc - atg
UL45+	79	atccttgtcgatcccgaaacgacacacgcgttgagcaaaaacgcctccctcgtgacgcgttctctatacaacaacaggc - atg
UL46-	43	ggcataactcgcaccggcggttcocgcacccgaacggcgctcacc - atg
UL47-	194	catttggccggggctggggcggttagcttcgcgggagatactgcgttttttgcgcggcccgctgcgtcccgctccat tccatcgcgaggggtccggcgccactaccocggcctccatcgcgcgtgtggggtcttttttttgggggtagcgga catcgcataaccgcgtctatcgccacc - atg
UL48-	179	cattctcgggaacggagcgggttcocgctgccacttcccccataaggtcgcgtccggtcctctaacgcgtttgggggtttct cttcccgcgctcgggcgccacactctctgtggcgggcggggacgatacgatcaaaagcccgatactgcttttccggtatcaaccocacca - atg
UL49-	150	gccactcagcatcccccagtggttttgcggaccctctctctccggggccgccctatcgtcgaccttccacacctgcacca cccccgcttcgaaacccaggcctaattgtcgcgcataccgacctagcgtgtctgtggaacc - atg
UL49A-	135	aggttcagttgcacgactccgccccgcgagtagcagcgcgtgtgccagtcgccatgtaacccccgaccccaag ctgtccgcttgacaagatgcgcccgatcccccactgactcatcttctgttagggacg - atg
UL50+	181	agacatttggccagtgtttgggtctgcacccgcgcgccccgcataccatcgcgcgcctctctcgcggcggtctcc cgcgcgggcccgcgtcccgctccgcgctaaggcgacagcagaagacaacaacagccccgcgcacagaccttctgtgggggccccatgcttaacagggaag - atg
UL51-	294	gccatttagcccgccgcagcgttgtagagcccgactctctcgaacctgtcttgcgttgggcccgtcggcaacggc catcgtgcgtgtatgctgtagctgaatatataaacccgctcgccccccagtagagatttgtgagggggcgatcgaaag aggtataaacgcaccgcgtcgtcgcataaagcgcggtcacctccacgggagtcgcgcgcgcctctcccccgcggtt cccgcttcttgcctccattgctgcgcgcgcccaaggccagtaaccgcgccg - atg
UL52+	63	acatatagccccagaaaagaagaagccatcgcggcggttacttgcccttggcgcgcggaacgca - atg
UL53+	236	agtaaggacgactgggtcctctacagctagtcctccgttcgcggttacctgcagcaaacctgtcgtgtcgtcgttt aagcacggccgggcgagtcgcgcacgcgcgcgaattcgtcgcgtgagcgtcggggccacaacccgctgtg cgtgtccttctgtacagtgctttgcgcgaatgcgacagaacccgcttcgacacgctgtttaccattgacgcgcggcacgcc - atg

Table 2 Continued

[illegible]

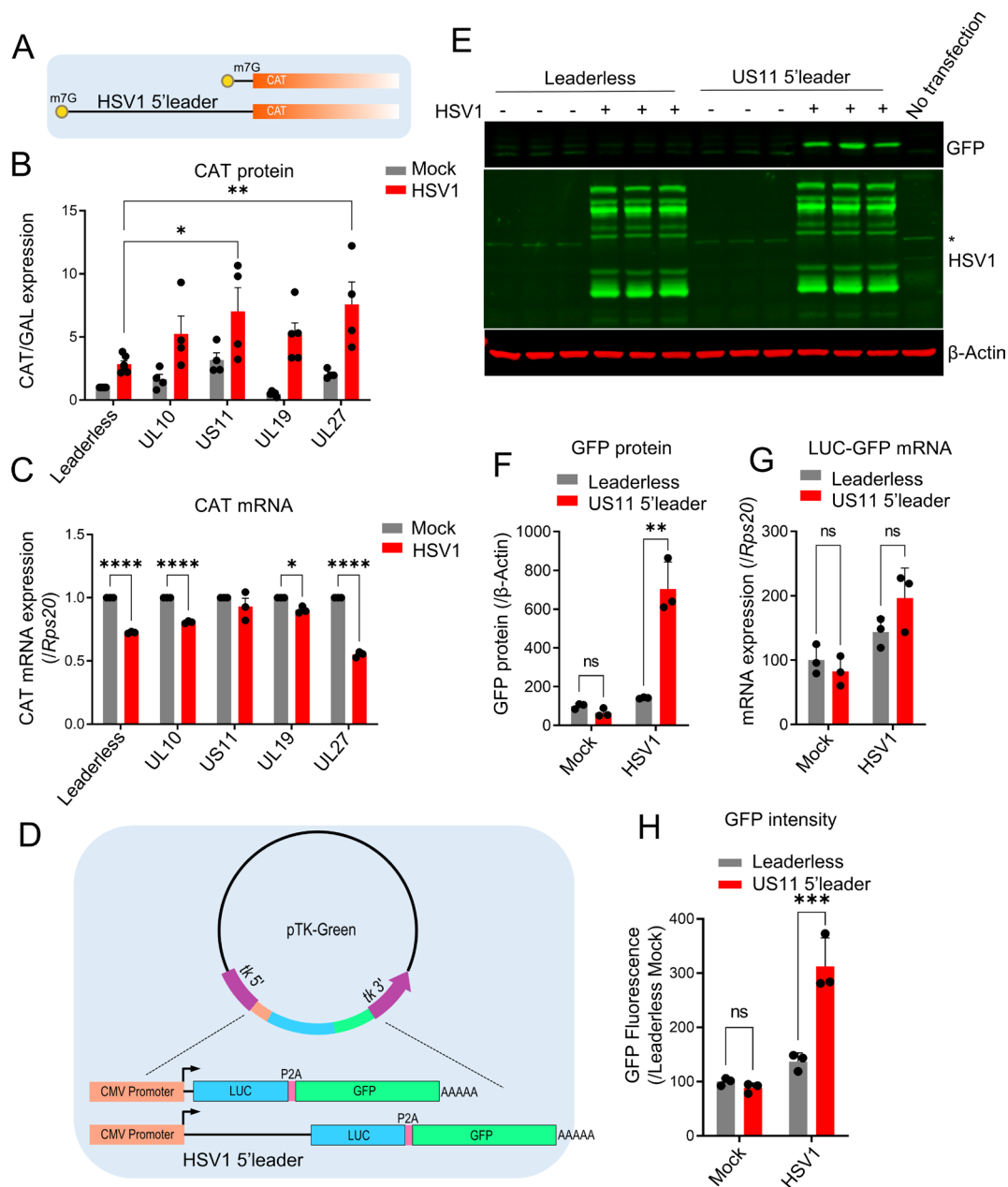
Continued

Table 2 Continued

Gene name (strand)	5'leader length	5'leader sequence
US8A+	118	acgtacattcgcgtgcccacagcgcagctgtacgcggactggagctcggacagcgaggagagaacgcgaccagg tcccggtgcgtgcccccccgagagacccgactctccctccacca - atg
US9+	65	agcaaattaaataatcgtgagtcacagcgaccgcaacttccacaccggagctttcttcggcctcg - atg
US10-	69	accocagaggtttcacgcacctcgcaggacaccgcgcgatctcoggaccocgcgaacggggtgata - atg
US11-	215	ggccagaacccgcgtgcacgacccggagcgtccctgtcgccttcccgggctgtgcccgaaatcg cccccaacgcatacttgggtgtggacatcagaacccggcggaccgtgaccgacagtcctcccgtaatcc ggtaacccgttgatccccgggtacgaccatcacccgagtcctctggtggcgagggtggttccccccgtgctctcgag - atg
US12-	486	gcagacggccgcgccacgaacgacgggagcggctgcggagcacgcggacccggagcggggagtcgcagagggcc gtcggagcggacggcgtcggcatcgcgacccccggctcggatcgggcatcgcatcggaaggacacgcggacgc gggggggaaagaccgcgccaccaccacgaacacaggggacgcaccccggggcctcgcgacgacagaaaacc accggtccgcctttttgcacggtgaagcaccttgggtggcggagaggggggacgcggggcgaggagggggg acgcgggggcgagaggggggacgcggggcggagaggggggacgcggggcgaggaggggggacgcggggg cggagaggggggtcaccccgcttcgtgccttccgcagagggaacgtcctcgtcgcgagcgacccggcgaccggttcggtg accgcttctcgtcgtcggggggagc - atg

5'leader was highest in augmenting the translation of CAT mRNA reporter. In contrast, the 5'leaders of UL1 and US8 were found to have none to inhibitory effects during HSV1 infection (online supplemental figure 4B). However, following HSV1 infection, we found that US11 and UL27 5'leaders significantly enhanced CAT protein expression (figure 2B) compared with the reporter lacking a leader (leaderless). Importantly, these observations are not through 5'leader-mediated upregulation of CAT mRNA transcription (figure 2C). We also predicted the folding free energy and potential secondary structure of the US11 and UL27 leaders (online supplemental figure 4C) and the folding free energy of other screened HSV1 leaders (online supplemental figure 4D). We found that despite having the strongest enhancement on CAT protein expression, the 5'leaders of US11 and UL27 have low predicted folding free energy compared with other HSV1 5'leaders. Together, these results suggest that the 5'leader sequences from US11 or UL27 mRNAs can mediate HSV1 infection-dependent increases in protein expression when inserted upstream of a transgene in cells.

Lytic infection by HSV1 induces a profound reprogramming of cellular transcription, splicing and nuclear export.<sup>41 43</sup> Thus, a plasmid-based overexpression reporter assay might be compromised by HSV1 infection and not faithfully reflect gene expression processes, including mRNA translation, of HSV1-encoded transgenes. Focusing on the US11 5'leader, we next investigated the effect of the US11 5'leader on regulating transgene expression directly from expression cassettes designed to be inserted within the *tk* locus of the HSV1 genome.<sup>27</sup> Briefly, transcription from the pTK plasmid expression cassette is driven by a CMV promoter and includes a SV40 polyadenylation signal (figure 2D). A bicistronic transgene cassette was created to allow concomitant expression of the therapeutic protein along with a reporter protein to facilitate recombinant virus selection and monitoring, all under the control of putative enhancer elements inserted at the 5'end of the expression cassette (figure 2D). The ORFs consist of luciferase (*luc*, which can be replaced with a desired therapeutic ORF) and *gfp* separated by the self-cleaving peptide porcine teschovirus-1 2A (P2A).<sup>44 45</sup> Western blot analysis of transfected cell lysates showed that inclusion of the US11 5'leader confers an increase in GFP protein levels in HSV1-infected cells (figure 2E,F). Consistent with our previous results, incorporation of the US11 5'leader did not affect levels of the *gfp* transcript in uninfected compared with HSV1-infected cells (figure 2G). GFP fluorescence was also quantified in 4T1 cells transfected with the leaderless plasmid or a plasmid harboring the US11 5'leader and subsequently infected with or without HSV1. Consistently, low fluorescence was observed in leaderless and uninfected cells, while HSV1 infection induced GFP fluorescence in the US11 5'leader construct (figure 2H).



**Figure 2** HSV1 US11 5'leader sequence enhances expression of protein reporters in HSV1-infected mammalian cells. (A) Schematic diagrams of the mRNAs expressed from CAT reporter construct without/with HSV1 5'leader. (B) Translation reporter assay to screen for HSV1 5'leader sequences that enhance translation during HSV1 infection. 4T1 cells were infected with HSV-1716-GFP at a MOI of 5, then transfected with the CAT plasmid and a  $\beta$ -GAL expression plasmid that serves as a transfection control. Cells were lysed 24 hours post-infection and CAT expression was quantified by ELISA, while  $\beta$ -GAL activity was quantified by colorimetric assay using ortho-Nitrophenyl- $\beta$ -galactoside substrate. Two-way ANOVA with Tukey's post-hoc test was performed. Only significant tests were shown. n=at least 3 biological replicates. Error bars:  $\pm$ SD \* $p$ <0.05, \*\* $p$ <0.01. (C) Relative CAT mRNA expression from CAT translation reporter assay. 4T1 cells were treated as in (B), then lysed using Trizol. RT-qPCR was then used to quantifie mRNA expression of CAT mRNA normalized to the expression of *Rps20*. Two-way ANOVA with Sidak's post-hoc test was performed. n=3 biological replicates. Error bars:  $\pm$ SD. \* $p$ <0.05, \*\* $p$ <0.01, \*\*\*\* $p$ <0.0001. (D) Schematic diagram of the pTK-Green plasmids that harbor the HSV1 5'leader-reporter construct for insertion into the HSV1 TK gene and the resulting transcripts. The ribosome skipping sequence P2A is inserted between the luciferase CDS and GFP CDS, which allowed for synthesis of 2 proteins from one cistron. (E) Western Blot of lysates from 293T cells that were treated as in (B) with antibodies against GFP, HSV1 or  $\beta$ -Actin. (\*): non-specific band. (F) Quantification of GFP expression from the Western Blots in (E). Two-way ANOVA with Sidak's post-hoc test was performed. n=3 biological replicates. Error bars:  $\pm$ SD. \* $p$ <0.05, \*\* $p$ <0.01, \*\*\*\* $p$ <0.0001. (G) RT-qPCR quantification of LUC-GFP mRNAs from the same experiment. Two-way ANOVA with Sidak's post-hoc test was performed. n=3 biological replicates. Error bars:  $\pm$ SD. \* $p$ <0.05, \*\* $p$ <0.01, \*\*\*\* $p$ <0.0001, ns, non-significant. (H) Quantification of GFP fluorescence. Cells were transfected with LUC-GFP reporter plasmid, then infected with the HSV1 (KOS strain) 4 hours post-transfection at a MOI of 2.5. Images were taken at 24 hours postinfection. ANOVA, analysis of variance; MOI, multiplicity of infection.



### The US11 5'leader enhances transgene protein expression from engineered HSV1 virions

To validate the potential of the US11 5'leader as a transgene enhancer, we constructed recombinant HSV1 strains based on the bicistronic pTK transgene expression plasmid described above. The linearized pTK plasmid can be used to generate recombinant viruses following cotransfection with purified HSV1 genomic DNA. Homologous recombination of the expression cassette into the *tk* locus produces  $\Delta tk$  virus progeny expressing the transgene in a constitutive manner under the CMV promoter (figure 3A). To better demonstrate the clinical potential, we replaced the *luc* ORF in the *luc-gfp* cassette with the *Csf2* (GM-CSF) ORF, a gene that is virally expressed in the FDA-approved oncolytic HSV1.<sup>46</sup> We generated a leaderless (HSV1 leaderless-*Csf2*) virus along with two virus clones incorporated with the US11 5'leader (HSV1 US11-*Csf2*) (figure 3B). In agreement with the enhanced expression of GFP conferred by the US11 5'leader in the plasmid-based systems, plaques on Vero cells of HSV1 US11-*Csf2* showed elevated GFP fluorescence compared with plaques of HSV1 *Csf2* (figure 3C). Cells infected with the HSV1 US11-*Csf2* virus produced ~7–8fold more GM-CSF compared with cells infected with HSV1 leaderless-*Csf2* (figure 3D, online supplemental figure 5). To assess if enhanced GM-CSF production is a result of higher viral replication, we measured replication kinetics by single-step growth curves and found that all virus clones exhibit comparable replication kinetics (figure 3E). RT-qPCR of mRNAs extracted from infected cells at various time points revealed that the presence of the 5'leader affected neither the expression kinetics of the HSV1 transcript US6 (figure 3F left panel) nor that of the transgene transcripts expressed in cis (*Csf2* and *gfp*, figure 3F middle and right panel) over the course of infection. To understand whether transgene-enhanced protein production might be a cell-type or species-dependent effect, we infected the human prostate cancer line DU145 and the human renal cell carcinoma line 786-O with wild-type, US11 5'leader, and leaderless viruses. Monitoring of GFP fluorescence intensity in these cells over the course of infection revealed a robust US11 5'leader-mediated enhancement of transgene protein expression in all cell lines tested (online supplemental figure 6). These results demonstrate the ability of the US11 5'leader to augment the production of a clinically relevant therapeutic transgene in HSV1-infected mammalian cells.

### The HSV1 US11 5'leader increases translational efficiency of associated transcript in a HSV1-dependent manner

We next sought to identify the mechanism underlying the increased expression of GM-CSF in cells infected with HSV1 US11-*Csf2*. We assessed whether the US11 5'leader has a bona fide effect on mRNA translation of the transgene by using the polysome profiling technique. Briefly, ribosome-bound mRNAs were separated by ultracentrifugation on a sucrose gradient, which causes mRNAs to sediment based on the number of bound ribosomes.

Accordingly, mRNAs that migrate toward heavier sucrose gradients have more bound ribosomes and higher translation efficiency. Vero cells were infected with HSV1 leaderless-*Csf2* or HSV1 US11-*Csf2* at a MOI of 5 (figure 4A), then the lysate containing ribosome-bound mRNAs was resolved on a 10%–50% sucrose gradient (figure 4B). We found that the presence of the US11 5'leader caused a shift of the *Csf2-gfp* transcript distribution toward heavier polysome fractions, demonstrating enhanced translation efficiency compared with the leaderless *Csf2-gfp* transcript (figure 4C,D). Interestingly, the *US6* and *US11* viral mRNAs are mostly distributed to the heavier polysome fractions (figure 4C,D), suggesting that HSV1 transcripts are generally highly translated despite the global shutoff of protein synthesis resulting from HSV1 infection.<sup>22</sup> Notably, without the US11 5'leader, the leaderless transgene *Csf2-gfp* mRNAs are suboptimally translated compared with the *US6* and *US11* viral mRNAs (online supplemental figure 7A,B). To address whether the translation enhancement mediated by the US11 5'leader is specific for HSV1 infected cells or a result of a general antiviral state, we tested GFP expression from the plasmid pTK-*Csf2-gfp* in Vero cells transfected with the dsRNA mimic poly(I:C) or infected with another virus, VSV. We observed that neither poly(I:C) transfection nor VSV infection were capable of inducing GFP expression (figure 4E). Thus, the enhancement of US11 5'leader on gene expression appears to be specific to HSV1 infected cells. These data suggest that traditional transgene cassettes that lack *cis*-acting translation enhancing elements are suboptimally translated when compared with HSV1 endogenous transcripts. These data also demonstrate that incorporation of the HSV1 US11 5'leader can significantly and specifically improve translation of HSV1-encoded transgenes.

### The US11 5'leader improves the antitumor effect of GM-CSF expressing HSV1 *in vivo*

A critical question is whether boosting the expression of a transgene beyond that achieved by current oncolytic HSV1 platforms ameliorates cancer outcomes. To answer this, we used the CT26 syngeneic tumor model of colon carcinoma that is routinely used to assess the efficacy of oncolytic HSV1.<sup>47,48</sup> Tumors were generated on both flanks of the mice, and tumor on one side was injected with resuspension buffer or  $5 \times 10^5$  viral particles of HSV1 leaderless-*Csf2* or HSV1 US11-*Csf2* (figure 5A). Incorporating the US11 5'leader enhanced the intratumoral GM-CSF protein expression in treated animals by more than twofold (figure 5B), while both viruses shared similar replication kinetics *in vivo* as shown by comparable transcription levels of the viral genes *US6* and *UL30* (figure 5C). This result suggests that while both viruses had similar infection rates, increased GM-CSF production was observed in HSV1 US11-*Csf2* infected tumors. GM-CSF is known to be a proinflammatory cytokine but might exert anti-inflammatory properties in certain contexts.<sup>49</sup> Thus, we probed the tumor microenvironment

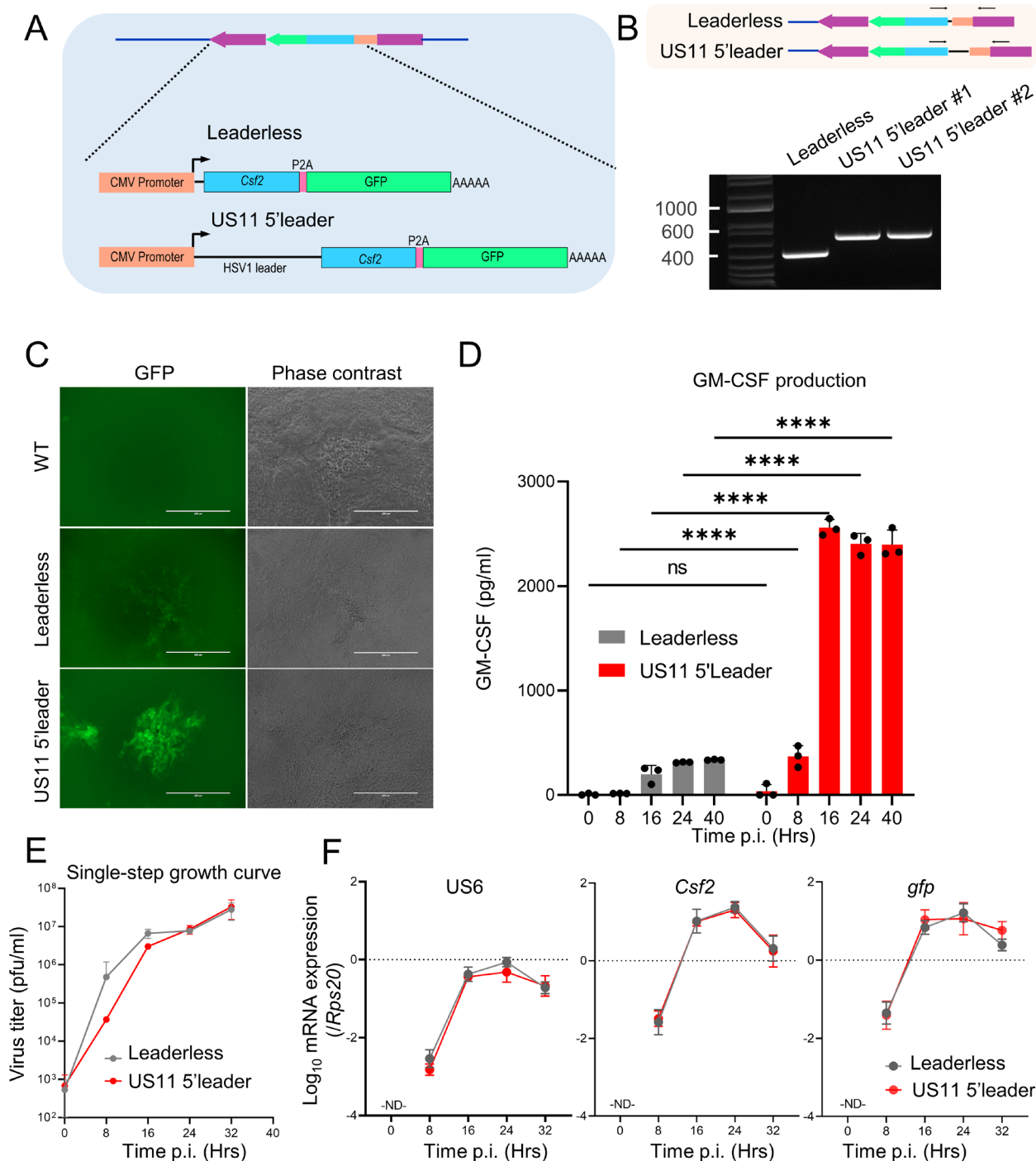


**Figure 3** A recombinant HSV1 virus exhibits a US11 5'leader-dependent boost in GM-CSF expression. (A) Schematic illustration of the expression cassette insertion scheme from the pTK-CSF2-GFP plasmid into HSV1 genome (note that the TK gene is on the minus strand), and the resulting transcripts expressed from the inserted cassette. (B) Virus genotyping for confirmation of expression cassette insertion. PCR was done using HSV1 gDNA extracted from purified viruses to confirm the insertion of the leaderless CSF2-GFP cassette (~400bp) and US11 5'leader-CSF2-GFP cassette (~600bp) into the TK region of HSV1 genome. (C) Fluorescence imaging of individual plaques of wild-type HSV1, HSV1 CsF2 and HSV1 US11-Csf2. (D) Quantification of GM-CSF production in culture supernatant of Vero cells infected with HSV1 expressing leaderless CSF2-GFP or US11 5'leader-CSF2-GFP. Monolayers of Vero cells were infected with the indicated virus at a MOI of 5, and the culture supernatant was collected 24 hours post-infection. GM-CSF concentration was quantified by ELISA. One-way ANOVA with Dunnett's post-hoc test was performed. n=3 biological replicates. Error bars:  $\pm$ SD. \*\*\*\*p<0.0001. (E) Single-step growth curve of HSV1 CsF2 and HSV1 US11-Csf2. Monolayers of Vero cells were infected at a MOI of 5, then intracellular and extracellular virus was collected and titrated at the indicated time points. (F) Transcription level of HSV1 endogenous gene (US6) and transgenes. Monolayers of Vero cells were infected at a MOI of 5, then cells were lysed using Trizol at the indicated time points. mRNA abundance was quantified by RT-qPCR and normalized to *Rps20*. ANOVA, analysis of variance. MOI, multiplicity of infection.

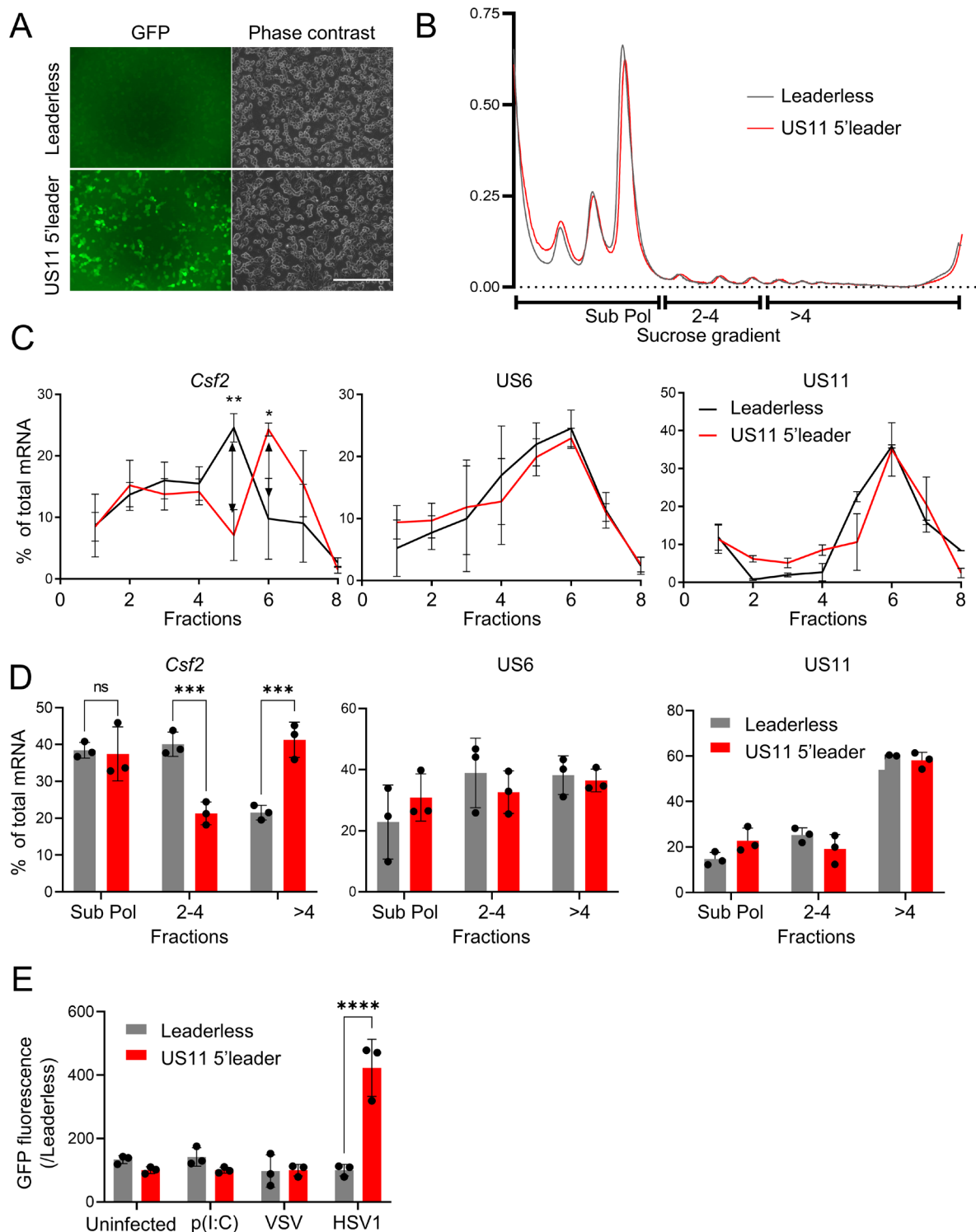


**Figure 4** The HSV1 US11 5'leader increases translation efficiency of a downstream transgene. (A) Fluorescence and phase contrast images of HSV1-infected Vero cells used for the polysome fractionation experiment in (B) and (C). scale bar: 400  $\mu$ m. (B) polysome traces of Vero cells infected with HSV1 Csf2 or HSV1 US11-Csf2 at a MOI of 5. Cells were lysed at 24 hours post-infection for polysome fractionation. (C) mRNA distribution in polysome fractions of Csf2 (left panel) and the endogenous HSV1 transcripts US6 (middle panel) and US11 (right panel), quantified by RT-qPCR. Two-tailed unpaired t-test was performed.  $n=3$  biological replicates. Error bars:  $\pm$ SD. \*\* $p<0.01$ , \* $p<0.05$ . (D) mRNA distribution in non-translating fractions (subpolysome), poorly translating fractions (2–4 ribosomes) and highly translating fractions (>4 ribosomes) of Csf2 (left panel), US6 (middle panel) and US11 (right panel) transcripts. Multiple unpaired  $t$ -test was performed.  $n=3$  biological replicates. Error bars:  $\pm$ SD. \*\*\*  $p<0.001$  (E) Quantification of GFP fluorescence of Vero cells transfected with pTK-CSF2-GFP plasmid with or without US11 leader sequence, co-transfected with poly(I:C) or infected immediately after with VSV or wild-type HSV1 at a MOI of 5. Two-way ANOVA with Sidak's post-hoc test was performed.  $n=3$  biological replicates. Error bars:  $\pm$ SD. \*\*\*\* $p<0.0001$ . ANOVA, analysis of variance. MOI, multiplicity of infection.

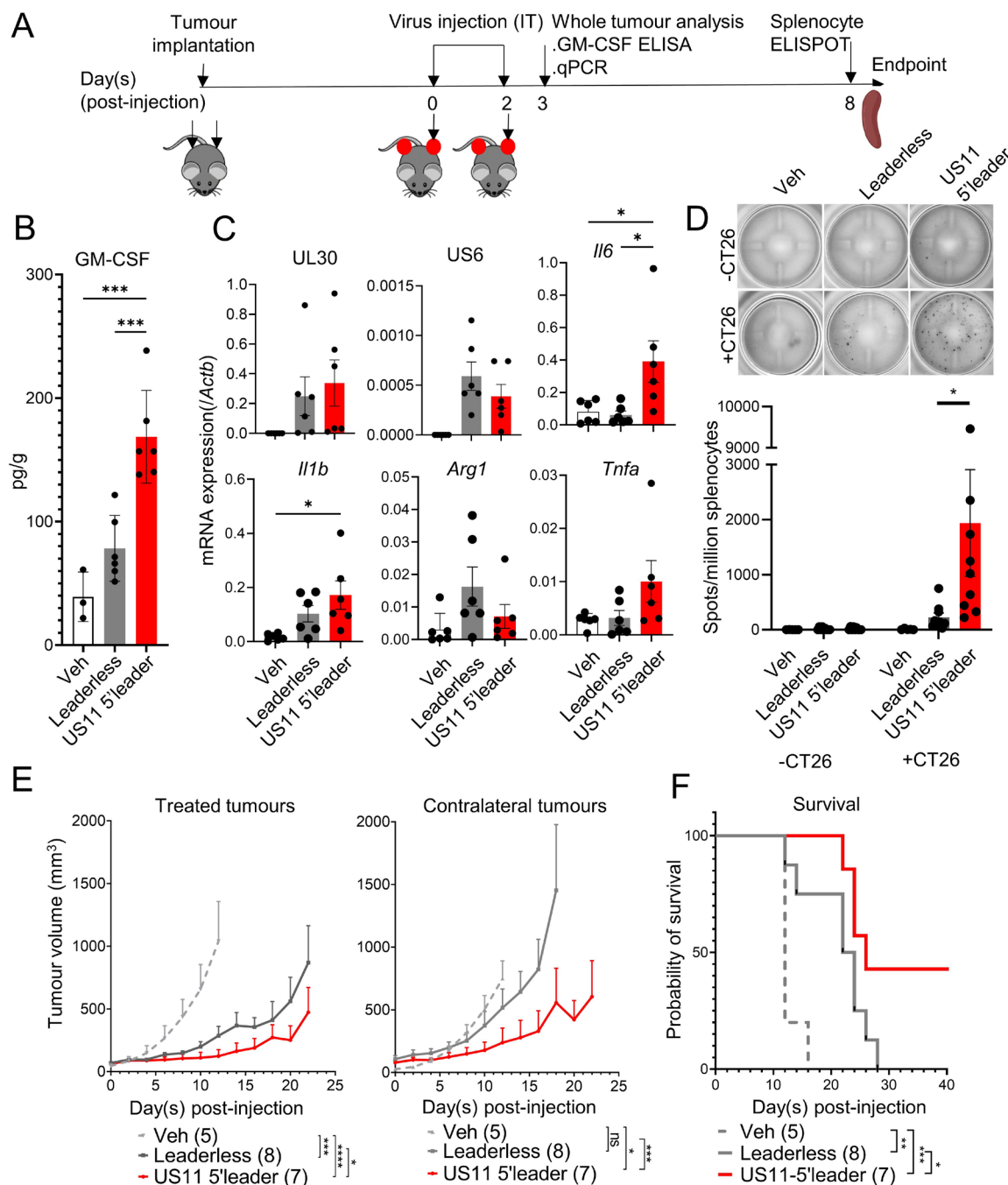


**Figure 5** US11 5'leader enhances the antitumor effect of GM-CSF expressing HSV1. (A) Schematic overview of the *in vivo* study to characterize the effect of HSV1 US11-Csf2 on tumor inflammation and systemic antitumor T-cells. 10<sup>5</sup> CT26 cells were injected in both flanks of BALB/c mice. When the tumor reached approximately 5×5 mm, two injections of 5×10<sup>5</sup> PFU of the indicated virus were performed intratumorally 2 days apart (day 0 and day 2). Tumor size was measured every 2 days. (B) Intratumoral GM-CSF level of tumor treated with leaderless or HSV1 US11-Csf2. Tumors as generated in (A) were excised 1 day after the second injection and homogenized in PBS. GM-CSF level was then quantified by ELISA. Two-tailed unpaired t-test was performed. n=3 biological replicates. Error bars: ±SD. \*\*\*p<0.001. (C) Viral transcripts and inflammatory genes expression level in oHSV1-treated tumors. RNA from tumors in (B) were extracted with Trizol, then mRNA abundance of the indicated transcripts were quantified by RT-qPCR and normalized to *Actb*. Two-tailed unpaired t-test was performed. n=3 biological replicates. Error bars: ±SD. \*p<0.05. (D) systemic tumor-specific T-cell responses after oHSV1 injection, evaluated by IFN $\gamma$  ELISPOT. Eight days after the first injection, splenocytes were isolated from mice, and co-cultured with/without UV-irradiated CT26 at a 2:1 responder-to-stimulator ratio for 24 hours. Representative ELISPOT wells are shown, as well as quantification of CT26-specific spots in the bar graph. Two-tailed unpaired t-test was performed. Error bars: ±SD. \*p<0.05. (E) the effect of Leaderless- or HSV1 US11-Csf2 treatment on tumor growth. Number of mice is shown in brackets. Two-way ANOVA with Tukey's post-hoc test was performed. Error bars: ±SD. \*p<0.05, \*\*\*p<0.001, \*\*\*\*p<0.0001. (F) Kaplan-Meier survival curve of mice treated with the Leaderless or US11-Csf2 HSV1. Number of mice is shown in brackets. \*p<0.05, \*\*p<0.01, \*\*\*p<0.001. ANOVA, analysis of variance.



of infected tumors by analyzing mRNA levels of representative inflammatory genes and found elevated levels of *Il1b*, *Il6*, and *Tnfa* mRNAs, and a statistically insignificant decrease of the immune suppressor gene *Arg1* in tumors treated with HSV1 US11-Csf2 (figure 5C). This observation suggests that HSV1 US11-Csf2 can induce a more inflammatory tumor microenvironment, even at the same treatment dose and growth rate as the leaderless virus. We also analyzed systemic antitumor response on the eighth day after the first injection by IFN $\gamma$  ELISPOT on splenocytes co-cultured with UV-irradiated CT26 cells. We found no CT-26-specific immune cell response in the spleen of vehicle-treated mice, while the leaderless HSV1 was capable of inducing a certain level of CT26-specific immune cells. However, the HSV1 US11-Csf2 induced a significantly higher CT26-specific T-cell response compared with the leaderless virus (figure 5D, online supplemental figure 8). Finally, we directly compared the antitumor effect of both viruses (figure 5E, online supplemental figure 9). As expected, regardless of viral clone, HSV1-injected tumors showed decreased growth relative to vehicle-injected tumors (figure 5F), a result consistent with the oncolytic and immunomodulatory properties of this viral platform.<sup>14 47 50</sup> Importantly, the growth of tumors injected with the US11 5'leader virus was significantly lower than that of tumors injected with the leaderless virus (figure 5F, left panel). More interestingly, treatment with the leaderless virus had no significant effect on the contralateral tumors, while treatment with the US11 5'leader virus significantly slowed tumor growth on the contralateral side, comparable to that observed in the treated one (figure 5F, right panel); suggesting an abscopal effect consistent with the elevated antitumor immune response observed by ELISPOT. Finally, we found that the US11 5'leader virus significantly improved mouse survival (figure 5G). Collectively, these data demonstrate that increasing the expression of GM-CSF via incorporation of the translation-enhancing US11 5'leader augments intratumoral cytokine production and boosts anticancer efficacy in a preclinical colon cancer model.

## DISCUSSION

In this work, we show that incorporating a HSV1 5'leader sequence enhances downstream transgene protein expression from a recombinant HSV1 virus. Our system tested for transgenes that are intracellular (CAT, LUC, GFP) or secreted (GM-CSF), and expression levels were consistently induced by the incorporation of the US11 5'leader during HSV1 infection. The elevated expression is mediated through increased mRNA translation of the modified transgene transcript within infected cancer cells. Importantly, we found that an oncolytic HSV1 harboring a 5'leader upstream of a therapeutic transgene has superior antitumor activity compared with a leaderless HSV1. This approach represents a simple yet highly effective way to improve the current generation of oncolytic HSV1

platforms that are presently in clinical trials. This strategy can be complementary to those that employ either a strong heterologous promoter to drive transgene expression, or an approach that inserts the transgene into a highly transcriptionally active region of the HSV1 genome. As an example of the former strategy, Toda *et al* found that a GM-CSF expression cassette driven by a CMV promoter and inserted into the TK region yielded approximately 55 pg of GM-CSF per 10<sup>5</sup> Vero cells.<sup>51</sup> In the present study, which also employed a CMV-driven GM-CSF expression cassette inserted in the TK region of the HSV1 genome, we saw 41.75 $\pm$ 2.35 pg GM-CSF per 10<sup>5</sup> Vero cells, a value very close to that previously reported (online supplemental figure 5A; calculated based on 167 $\pm$ 9.4 pg/mL of GM-CSF observed in a 12-well plate format at confluency, which typically contains 4 $\times$ 10<sup>5</sup> cells in 1 mL of culture media). Yet, with the introduction of the US11 5'leader, close to an eight-fold increase in GM-CSF production was obtained, representing a significant improvement in transgene protein expression. It is possible that transgene production could be improved even further by combining a strong HSV1 promoter (e.g., the one driving HSV1 RL2 expression)<sup>47 52</sup> with a translation enhancer found in viral 5'leaders and potentially also viral 3'UTRs. Additionally, minimal translation enhancing motif(s) specific for HSV1 infection could provide less recombination risk than full length 5'leaders, especially if to be applied to a novel generation of oncolytic HSV1 encoding for multiple therapeutic transgenes.

We have found that the enhanced translation of *Csf2* transcript expressed from a HSV1 backbone improved antitumor efficacy in a dual transplanted flank mouse cancer model. As expected, tumors treated with the leaderless-Csf2 HSV1 had slower progression, and the corresponding mice had a better survival rate compared with mock-treated counterparts (figure 5F,G). However, the HSV1 US11-Csf2 virus not only inhibited tumor growth to a greater extent in the injected side, but also induced significant growth inhibition in the contralateral tumors and resulted in a further improved survival rate. Consistently, we observed a higher intratumoral GM-CSF concentration in tumors from mice administered the US11 5'leader HSV1, which also correlated with upregulation of proinflammatory genes (figure 5B,D) and elevated levels of tumor-specific immune cells in the spleens of treated mice (figure 5D), suggesting a modification of the tumor microenvironment toward a desired inflammatory milieu that resulted from an augmented anticancer immune response. As GM-CSF was previously shown to enhance systemic antitumor immune responses,<sup>53</sup> our data indicate that an increase in GM-CSF production can induce a more inflammatory tumor microenvironment and lead to an improved systemic anticancer immune response against distant tumors. Overall, our data show that the use of a strong promoter (CMV promoter) alone does not maximize transgene protein expression, but that incorporation of a translation enhancer can boost the payload levels further, leading to increased oncolytic virus efficacy.

The findings presented herein identified *cis*-acting sequences within virus-based therapies that can be exploited to enhance transgene protein expression. The method was first conceptualized by the comprehensive annotation of viral 5' leader sequences through TSS identification by RNA-Seq and mapping translational efficiency across a viral genome by ribosome profiling. During the lytic cycle, HSV1 expresses its genes in an orderly manner, classified into immediate-early (ie), early (E), and late (L) genes.<sup>54</sup> We screened for selected 5' leaders that are highly expressed in the late stage of HSV1 infection and thus might also be better tuned to enhance translation at this stage of infection (figure 2). Our mini-screen did not cover all HSV1 5' leaders; thus, there might be other specific viral sequences with potentially superior translation enhancing activity at a different time of infection that could be revealed with a more comprehensive study of all HSV1 5' leaders. This study provides an impetus to investigate whether HSV1 5' leaders mediate an additional layer of temporal regulation on HSV1 gene expression by translational regulation.

We have shown here that the HSV1 US11 5' leader sequence fused upstream of transgenes encoded within HSV1 can be used to enhance therapeutic payload expression and improve the antitumor efficacy of the virus. Our study exemplifies a novel method for optimizing the expression level of a desired transgene that can be applied to other virus-based therapeutic contexts. These findings also invite further studies to better understand post-transcriptional gene expression in perturbed cellular conditions, such as in virally infected cells.

#### Author affiliations

<sup>1</sup>Children's Hospital of Eastern Ontario Research Institute, Ottawa, Ontario, Canada

<sup>2</sup>Department of Biochemistry, Microbiology, and Immunology, University of Ottawa, Ottawa, Ontario, Canada

<sup>3</sup>Centre for Infection, Immunity and Inflammation, University of Ottawa Faculty of Medicine, Ottawa, Ontario, Canada

<sup>4</sup>Department Immunology, University of Toronto, Toronto, Ontario, Canada

<sup>5</sup>Department of Biomedicine, Aarhus University, Aarhus, Denmark

<sup>6</sup>Department of Medicine, McMaster University, Hamilton, Ontario, Canada

<sup>7</sup>Patrick G. Johnston Centre for Cancer Research, Queen's University Belfast, Belfast, UK

<sup>8</sup>Department of Pathobiology, University of Guelph, Guelph, Ontario, Canada

**Twitter** Samuel T Workenhe @samworkenhe and Tommy Alain @tommyalain3

**Contributors** All authors contributed to the data analysis and interpretation, drafting and revising of the manuscript, and provided final approval to submit the manuscript for publication. Guarantor author: TA.

**Funding** H-DH is a recipient of a University of Ottawa Graduate Scholarship, an Ontario Graduate Scholarship, and a University of Ottawa Faculty of Medicine Destination 2020 Scholarship. This work was supported in part by a Terry Fox Research Institute New Project Grant for TA and TEG, a Canadian Cancer Society Research Institute Innovation to Impact Grant (#706852) and Canadian Institute of Health Research (CIHR) bridge funding to TA, TEG and H-DH, a Natural Sciences and Engineering Research Council (NSERC) Discovery grant and Cancer Research Society grant to TA, and a Canadian Breast Cancer Foundation—Ontario Node grant to TA and TEG. DO was supported by the Lundbeckfonden (R335-2019-2138), the Novonordiskfonden (NNF220C0079512), and Kræftens Bekæmpelse (R279-A16218).

**Competing interests** H-DH, TEG, and TA are inventors on a provisional patent application regarding the use of US11 5' leader in oncolytic HSV1.

**Patient consent for publication** Not applicable.

**Ethics approval** All animal procedures were approved by the University of Ottawa Animal Care Committee.

**Provenance and peer review** Not commissioned; externally peer reviewed.

**Data availability statement** Data are available in a public, open access repository. Data are available on reasonable request. The RNA-seq data were published previously and are available on the NCBI Gene Expression Omnibus (GEO: GSE137757), sample IDs GSM4086602 and GSM4086610 (HSV1 infected mRNA replicate).

**Supplemental material** This content has been supplied by the author(s). It has not been vetted by BMJ Publishing Group Limited (BMJ) and may not have been peer-reviewed. Any opinions or recommendations discussed are solely those of the author(s) and are not endorsed by BMJ. BMJ disclaims all liability and responsibility arising from any reliance placed on the content. Where the content includes any translated material, BMJ does not warrant the accuracy and reliability of the translations (including but not limited to local regulations, clinical guidelines, terminology, drug names and drug dosages), and is not responsible for any error and/or omissions arising from translation and adaptation or otherwise.

**Open access** This is an open access article distributed in accordance with the Creative Commons Attribution Non Commercial (CC BY-NC 4.0) license, which permits others to distribute, remix, adapt, build upon this work non-commercially, and license their derivative works on different terms, provided the original work is properly cited, appropriate credit is given, any changes made indicated, and the use is non-commercial. See <http://creativecommons.org/licenses/by-nc/4.0/>.

#### ORCID iDs

Samuel T Workenhe <http://orcid.org/0000-0001-9521-3903>

Tommy Alain <http://orcid.org/0000-0002-0396-9138>

#### REFERENCES

- 1 Rauch S, Jasny E, Schmidt KE, *et al.* New vaccine technologies to combat outbreak situations. *Front Immunol* 2018;9:1963.
- 2 Macedo N, Miller DM, Haq R, *et al.* Clinical landscape of oncolytic virus research in 2020. *J Immunother Cancer* 2020;8:e001486.
- 3 Bulcha JT, Wang Y, Ma H, *et al.* Viral vector platforms within the gene therapy landscape. *Signal Transduct Target Ther* 2021;6:53.
- 4 Serafini P, Carbley R, Noonan KA, *et al.* High-Dose granulocyte-macrophage colony-stimulating factor-producing vaccines impair the immune response through the recruitment of myeloid suppressor cells. *Cancer Res* 2004;64:6337–43.
- 5 Conner J, Braidwood L. Expression of inhibitor of growth 4 by HSV1716 improves oncolytic potency and enhances efficacy. *Cancer Gene Ther* 2012;19:499–507.
- 6 Pearl TM, Markert JM, Cassidy KA, *et al.* Oncolytic virus-based cytokine expression to improve immune activity in brain and solid tumors. *Mol Ther Oncolytics* 2019;13:14–21.
- 7 Zhang Q, Liu F. Correction: advances and potential pitfalls of oncolytic viruses expressing immunomodulatory transgene therapy for malignant gliomas. *Cell Death Dis* 2020;11:1007.
- 8 Zheng M, Huang J, Tong A, *et al.* Oncolytic viruses for cancer therapy: barriers and recent advances. *Mol Ther Oncolytics* 2019;15:234–47.
- 9 Todo T, Ito H, Ino Y, *et al.* Intratumoral oncolytic herpes virus G47Δ for residual or recurrent glioblastoma: a phase 2 trial. *Nat Med* 2022;28:1630–9.
- 10 Todo T, Ino Y, Ohtsu H, *et al.* A phase I/II study of triple-mutated oncolytic herpes virus G47Δ in patients with progressive glioblastoma. *Nat Commun* 2022;13:4119.
- 11 Cripe TP, Chen C-Y, Denton NL, *et al.* Pediatric cancer gone viral. part I: strategies for utilizing oncolytic herpes simplex virus-1 in children. *Mol Ther Oncolytics* 2015;2:15015.
- 12 Walsh D, Mohr I. Viral subversion of the host protein synthesis machinery. *Nat Rev Microbiol* 2011;9:860–75.
- 13 Hoang H-D, Graber TE, Alain T. Battling for ribosomes: translational control at the forefront of the antiviral response. *J Mol Biol* 2018;430:1965–92.
- 14 Hu JCC, Coffin RS, Davis CJ, *et al.* A phase I study of oncovexgm-CSF, a second-generation oncolytic herpes simplex virus expressing granulocyte macrophage colony-stimulating factor. *Clin Cancer Res* 2006;12:6737–47.
- 15 Breitbach CJ, Burke J, Jonker D, *et al.* Intravenous delivery of a multi-mechanistic cancer-targeted oncolytic poxvirus in humans. *Nature* 2011;477:99–102.

- 16 Dhungel P, Cao S, Yang Z. The 5'-poly (a) leader of poxvirus mrna confers a translational advantage that can be achieved in cells with impaired cap-dependent translation. *PLoS Pathog* 2017;13:e1006602.
- 17 Jha S, Rollins MG, Fuchs G, *et al.* Trans-kingdom mimicry underlies ribosome customization by a poxvirus kinase. *Nature* 2017;546:651–5.
- 18 Mears WE, Rice SA. The RGG box motif of the herpes simplex virus ICP27 protein mediates an RNA-binding activity and determines in vivo methylation. *J Virol* 1996;70:7445–53.
- 19 Sandri-Goldin RM. Icp27 mediates HSV RNA export by shuttling through a leucine-rich nuclear export signal and binding viral intronless RNAs through an RGG motif. *Genes Dev* 1998;12:868–79.
- 20 Rivera AA, Wang M, Suzuki K, *et al.* Mode of transgene expression after fusion to early or late viral genes of a conditionally replicating adenovirus via an optimized internal ribosome entry site in vitro and in vivo. *Virology* 2004;320:121–34.
- 21 Liu BL, Robinson M, Han Z-Q, *et al.* Icp34.5 deleted herpes simplex virus with enhanced oncolytic, immune stimulating, and anti-tumour properties. *Gene Ther* 2003;10:292–303.
- 22 Hoang H-D, Graber TE, Jia J-J, *et al.* Induction of an alternative mRNA 5' leader enhances translation of the ciliopathy gene INPP5E and resistance to oncolytic virus infection. *Cell Rep* 2019;29:4010–23.
- 23 Kim D, Langmead B, Salzberg SL. HISAT: a fast spliced aligner with low memory requirements. *Nat Methods* 2015;12:357–60.
- 24 Afgan E, Baker D, Batut B, *et al.* The galaxy platform for accessible, reproducible and collaborative biomedical analyses: 2018 update. *Nucleic Acids Res* 2018;46:W537–44.
- 25 Trapnell C, Williams BA, Pertea G, *et al.* Transcript assembly and quantification by RNA-seq reveals unannotated transcripts and isoform switching during cell differentiation. *Nat Biotechnol* 2010;28:511–5.
- 26 Graber TE, Baird SD, Kao PN, *et al.* Nf45 functions as an IRES trans-acting factor that is required for translation of cIAP1 during the unfolded protein response. *Cell Death Differ* 2010;17:719–29.
- 27 Minaker RL, Mossman KL, Smiley JR. Functional inaccessibility of quiescent herpes simplex virus genomes. *Virol J* 2005;2:85.
- 28 Gandin V, Sikström K, Alain T, *et al.* Polysome fractionation and analysis of mammalian translomes on a genome-wide scale. *J Vis Exp* 2014;1–9.
- 29 Bommarreddy PK, Peters C, Saha D, *et al.* Oncolytic herpes simplex viruses as a paradigm for the treatment of cancer. *Annu Rev Cancer Biol* 2018;2:155–73.
- 30 Huang CJ, Wagner EK. The herpes simplex virus type 1 major capsid protein (VP5-UL19) promoter contains two cis-acting elements influencing late expression. *J Virol* 1994;68:5738–47.
- 31 Steffy KR, Weir JP. Upstream promoter elements of the herpes simplex virus type 1 glycoprotein H gene. *J Virol* 1991;65:972–5.
- 32 Pederson NE, Person S, Homa FL. Analysis of the GB promoter of herpes simplex virus type 1: high-level expression requires both an 89-base-pair promoter fragment and a nontranslated leader sequence. *J Virol* 1992;66:6226–32.
- 33 Goodart SA, Guzowski JF, Rice MK, *et al.* Effect of genomic location on expression of beta-galactosidase mRNA controlled by the herpes simplex virus type 1 UL38 promoter. *J Virol* 1992;66:2973–81.
- 34 Mavromara-Nazos P, Roizman B. Delineation of regulatory domains of early (beta) and late (gamma 2) genes by construction of chimeric genes expressed in herpes simplex virus 1 genomes. *Proc Natl Acad Sci U S A* 1989;86:4071–5.
- 35 Rixon FJ, Clements JB. Detailed structural analysis of two spliced HSV-1 immediate-early mRNAs. *Nucleic Acids Res* 1982;10:2241–56.
- 36 Greco A, Simonin D, Diaz JJ, *et al.* The DNA sequence coding for the 5' untranslated region of herpes simplex virus type 1 ICP22 mRNA mediates a high level of gene expression. *J Gen Virol* 1994;75 (Pt 7):1693–702.
- 37 Tang S, Patel A, Krause PR. Hidden regulation of herpes simplex virus 1 pre-mRNA splicing and polyadenylation by virally encoded immediate early gene ICP27. *PLOS Pathog* 2019;15:e1007884.
- 38 Tombácz D, Csabai Z, Szűcs A, *et al.* Long-read isoform sequencing reveals a hidden complexity of the transcriptional landscape of herpes simplex virus type 1. *Front Microbiol* 2017;8:1079.
- 39 Tombácz D, Moldován N, Balázs Z, *et al.* Multiple long-read sequencing survey of herpes simplex virus dynamic transcriptome. *Front Genet* 2019;10:834.
- 40 Whisnant AW, Jürges CS, Hennig T, *et al.* Integrative functional genomics decodes herpes simplex virus 1. *Nat Commun* 2020;11:2038:2038..
- 41 Rutkowski AJ, Erhard F, L'Hernault A, *et al.* Widespread disruption of host transcription termination in HSV-1 infection. *Nat Commun* 2015;6:7126:7126..
- 42 Zhao TT, Graber TE, Jordan LE, *et al.* Hnnp A1 regulates UV-induced NF-kappaB signalling through destabilization of cIAP1 mRNA. *Cell Death Differ* 2009;16:244–52.
- 43 Tang S, Patel A, Krause PR. Herpes simplex virus ICP27 regulates alternative pre-mRNA polyadenylation and splicing in a sequence-dependent manner. *Proc Natl Acad Sci U S A* 2016;113:12256–61.
- 44 Donnelly MLL, Luke G, Mehrotra A, *et al.* Analysis of the aphthovirus 2A/2B polyprotein “cleavage” mechanism indicates not a proteolytic reaction, but a novel translational effect: a putative ribosomal “SKIP.” *J Gen Virol* 2001;82:1013–25.
- 45 Kim JH, Lee S-R, Li L-H, *et al.* High cleavage efficiency of a 2A peptide derived from porcine teschovirus-1 in human cell lines, zebrafish and mice. *PLoS One* 2011;6:e18556.
- 46 Pol J, Kroemer G, Galluzzi L. First oncolytic virus Approved for melanoma immunotherapy. *Oncoimmunology* 2016;5:e1115641.
- 47 Malhotra S, Kim T, Zager J, *et al.* Use of an oncolytic virus secreting GM-CSF as combined oncolytic and immunotherapy for treatment of colorectal and hepatic adenocarcinomas. *Surgery* 2007;141:520–9.
- 48 Moesta AK, Cooke K, Piasecki J, *et al.* Local delivery of oncovexmgm-CSF generates systemic antitumor immune responses enhanced by cytotoxic T-lymphocyte-associated protein blockade. *Clin Cancer Res* 2017;23:6190–202.
- 49 Bhattacharya P, Budnick I, Singh M, *et al.* Dual role of GM-CSF as a pro-inflammatory and a regulatory cytokine: implications for immune therapy. *J Interferon Cytokine Res* 2015;35:585–99.
- 50 Kim K-J, Moon D, Kong SJ, *et al.* Antitumor effects of IL-12 and GM-CSF co-expressed in an engineered oncolytic HSV-1. *Gene Ther* 2021;28:186–98.
- 51 Toda M, Martuza RL, Rabkin SD. Tumor growth inhibition by intratumoral inoculation of defective herpes simplex virus vectors expressing granulocyte-macrophage colony-stimulating factor. *Mol Ther* 2000;2:324–9.
- 52 Thomas S, Kuncheria L, Roulstone V, *et al.* Development of a new fusion-enhanced oncolytic immunotherapy platform based on herpes simplex virus type 1. *J Immunother Cancer* 2019;7:214.
- 53 Yan WL, Shen KY, Tien CY, *et al.* Recent progress in GM-CSF-based cancer immunotherapy. *Immunotherapy* 2017;9:347–60.
- 54 Honess RW, Roizman B. Regulation of herpesvirus macromolecular synthesis. I. cascade regulation of the synthesis of three groups of viral proteins. *J Virol* 1974;14:8–19.